Magnetohydrodynamic turbulence in warped accretion discs

Ulf Torkelsson[*], Gordon I. Ogilvie[†], Axel Brandenburg[‡], James E. Pringle[†], Åke Nordlund[‖], Robert F. Stein[¶]

[*]*Chalmers University of Technology/Göteborg University, Department of Astronomy and Astrophysics, S-412 96 Gothenburg, Sweden*
[†]*Institute of Astronomy, Madingley Road, Cambridge CB3 0HA, United Kingdom*
[‡]*Department of Mathematics, University of Newcastle upon Tyne, NE1 7RU, United Kingdom, Nordita, Blegdamsvej 17, DK-2100 Copenhagen Ø, Denmark*
[‖]*Theoretical Astrophysics Center, Juliane Maries Vej 30, DK-2100 Copenhagen Ø, Denmark, Copenhagen University Observatory, Juliane Maries Vej 30, DK-2100*
[¶]*Department of Physics and Astronomy, Michigan State University, East Lansing, MI 48824, USA*

Abstract. Warped, precessing accretion discs appear in a range of astrophysical systems, for instance the X-ray binary Her X-1 and in the active nucleus of NGC4258. In a warped accretion disc there are horizontal pressure gradients that drive an epicyclic motion. We have studied the interaction of this epicyclic motion with the magneto-hydrodynamic turbulence in numerical simulations. We find that the turbulent stress acting on the epicyclic motion is comparable in size to the stress that drives the accretion, however an important ingredient in the damping of the epicyclic motion is its parametric decay into inertial waves.

I INTRODUCTION

Warped accretion discs have been a part of the astronomical vocabulary since the discovery of the 35-day cycle of the X-ray binary Her X-1 [1–3]. Incidentally Her X-1 was the first occulting X-ray pulsar for which an optical counterpart was found as discussed by Neta Bahcall at the 6th Texas Symposium in 1972 [4]. Later on warped accretion discs have been found in a multitude of systems. In later years one of the most interesting examples has been the maser source in the active galactic nucleus of NGC 4258 [5].

While the warped accretion disc offered a simple interpretation of the observations, it was not easy to describe it theoretically at the hydrodynamic level. The problems have been both to explain the excitation mechanism of the warp and its coherence. Pringle [6] showed that the radiation pressure from the central radiation source may produce a warp in the outer disc, and Schandl & Meyer [7] described

arXiv:astro-ph/0103057v1 3 Mar 2001

a similar mechanism in which the irradiation produces a wind, which in its turn excites a warp.

A crucial condition for any of these mechanisms to work is that the tendency of the disc to straighten itself must be sufficiently weak. There are two different forces that strive to produce a flat disc. Firstly there is the usual viscous stress due to the local turbulence, which is also driving the accretion, but in general it is insignificant compared to the hydrodynamic stress due to the epicyclic shear flow which is driven by the warp itself [8,9]. The amplitude of the epicyclic motion is inversely proportional to the ordinary turbulent viscosity. For that reason the hydrodynamic stress due to the epicyclic motion will also be inversely proportional to the turbulent viscosity, and the time scale for flattening the disc will be anomalously short compared to the ordinary viscous time scale.

The warping instability therefore requires a mechanism that can damp the epicyclic motion much more efficiently than it transports the angular momentum in the radial direction. That would for instance be the case if the turbulent viscosity was strongly anisotropic. The intention of this paper is to estimate how anisotropic the turbulent viscosity is and to check whether there are any other mechanisms that can limit the amplitude of the epicyclic motion. We describe the numerical model that we use for these estimates in Sect. 2. There are then two ways in which we have studied the interaction between the turbulence and the epicyclic motion. Firstly we have studied the free decay of an epicyclic motion (Sect. 3) and secondly we have studied the motion that results from a radial forcing (Sect. 4). We discuss and summarize our results in Sect. 5.

II   THE MATHEMATICAL MODEL

We solve the magnetohydrodynamical equations in a Keplerian shearing box [10–12]. Our units are chosen such that $H = GM = \mu_0 = 1$, where G is the gravitational constant, M the mass of the central object, and H is the Gaussian scale height of the shearing box. The density distribution assuming isothermality can then be written as $\rho = \rho_0 e^{-z^2/H^2}$, where we put $\rho_0 = 1$. The physical size of the shearing box is $L_x : L_y : L_z = 1 : 2\pi : 4$, and the box is positioned such that x and z vary between $\pm\frac{1}{2}L_x$, and $\pm\frac{1}{2}L_z$, respectively, while y goes from 0 to L_y, and the distance of the origin to the central object, $R_0 = 10$. This gives the orbital period $T_0 = 199$, and the mean internal energy $e_0 = 7.4\,10^{-4}$. To stop the box from heating up we add a cooling function

$$Q = -\sigma_{\mathrm{cool}}\left(e - e_0\right), \qquad (1)$$

where σ_{cool} is the cooling rate, which typically corresponds to a time scale of 1.5 orbital periods. Our boundary conditions are (sliding) periodic in the (x-) y-direction. In the z-direction they are impenetrable and stress-free for the velocity, and acts as a perfect conductor with respect to the magnetic field.
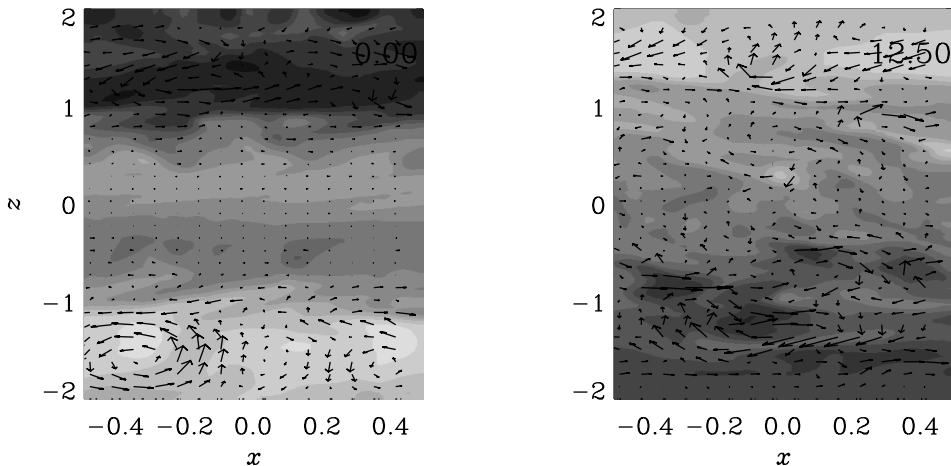
FIGURE 1. The magnetic field in a meridional cut of the simulation at the beginning of the simulation (left) and after 12.5 orbital periods (right). The toroidal field is plotted using a grey scale and the poloidal field as vectors. Note that the toroidal field has been reversed between the two images.

We start the simulations from a snapshot from a previous simulation in which the magnetohydrodynamic turbulence is already fully developed. In the first set of simulations we then add a radial velocity of the form $u_x = u_0 \sin(\pi z/L_z)$, which will have the time evolution of an epicyclic motion. In the second set of simulations, we do not modify the velocity field of the initial snapshot, but rather add a radial forcing term to the equation of motion. This forcing gives an acceleration with a harmonic time-dependence on the orbital time scale and the same z-dependence as the velocity above.

III   THE FREE DECAY OF AN EPICYCLIC MOTION

In the first set of simulations we add an epicyclic motion to the initial state of the simulation, and then follow the decay of the epicyclic motion. These simulations have previously been described in [13]. With a weak epicyclic motion, its maximum Mach number is initially 0.38, it is difficult to follow the evolution of the epicyclic motion as it is comparable in size to the turbulent velocities. When the amplitude is increased to a Mach number of 3.3, we can distinguish two stages in the damping. After a brief period of essentially no damping the epicyclic velocity quickly drops by a factor of 2 to 3. This damping is followed by an extended phase of exponential decay with a time scale of 25 orbital periods. The time scale of the exponential decay can be translated to a Shakura-Sunyaev [14] α-parameter of 0.006, which is within a factor of two of the values usually derived from turbulence simulations, e.g. [10,15]. The preceding rapid damping is a new phenomenon though, which we interpret in terms of that the epicyclic motion is decaying to inertial waves
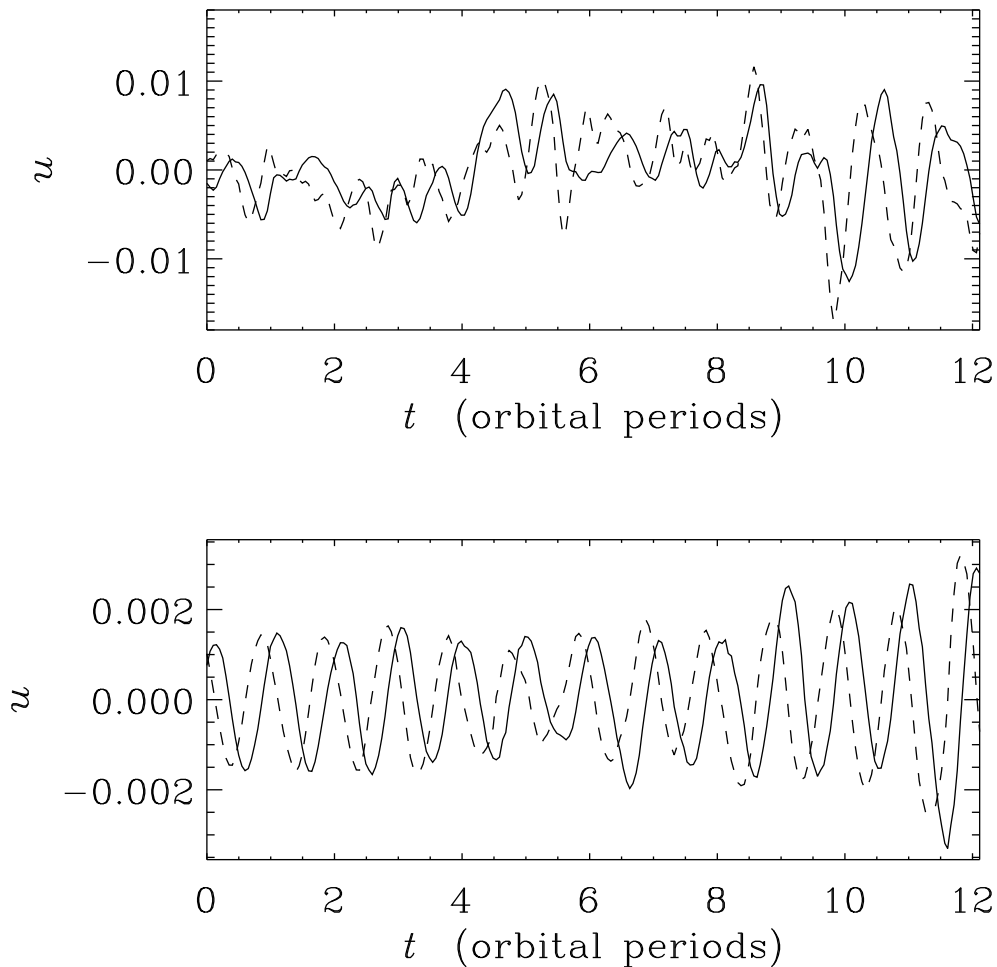
FIGURE 2. $\langle u_x \rangle$ (solid line) and $2\langle u_y \rangle$ (dashed line) as functions of time at $z = 1.17$ (top) and $z = -0.25$ (bottom).

via a parametric instability [16]. We also note that the toroidal magnetic field in the shearing box reverses its direction during the damping of the strong epicyclic motion (Fig. 1).

IV DRIVEN EPICYCLIC MOTION

The dynamics in a real accretion disc is significantly different from the case we have studied above. In reality the epicyclic motion will be driven by the radial pressure gradient that is set up by the warp. To mimic this we have carried out a new set of simulations in which we drive the epicyclic motion by adding a time-periodic radial force to the equation of motion.

We plot the horizontally averaged velocities $\langle u_x \rangle$ and $\langle u_y \rangle$ in Fig. 2. The epicyclic motion is in this case comparable to that of Run 1b in [13]. The results are similar in the two cases, and the epicyclic motion is difficult to distinguish at $z = 1.17$ due to the effect of the turbulent stresses, while it is easily distinguishable at $z = -0.29$.

V   CONCLUSIONS

In this paper we have studied the dynamics of an epicyclic flow in a Keplerian shear flow. In our simulations we find two damping mechanisms for the epicyclic motion. The turbulent stresses can damp the motion in a way which can be described in terms of a turbulent viscosity comparable in strength to that driving the radial angular momentum transport, but a sufficiently fast epicyclic motion can lose significant amounts of energy by exciting inertial waves through a parametric instability.

ACKNOWLEDGMENTS

REFERENCES

1. Tananbaum, H., Gursky, H., Kellogg, E. M., Levinson, R., Schreier, E.,, Giacconi, R., *ApJ*, **174**, L143–L149 (1972)
2. Katz, J. L., *Nat. Phys. Sci.*, **246**, 87–89 (1973)
3. Roberts, W. J., *ApJ*, **187**, 575–584 (1974)
4. Bahcall, N. A., "Optical Observations of HZ Herculis", in *Sixth Texas Symposium on Relativistic Astrophysics*, edited by D. J. Hegyi, Ann. N. Y. Acad. Sci. 224, New York, 1973, pp. 178–183
5. Miyoshi, M., Moran, J., Herrnstein, J., Greenhill, L., Nakai, N., Diamond, P.,, Inoue, M., *Nat*, **373**, 127–129 (1995)
6. Pringle, J. E., *MNRAS*, **281**, 357–361 (1996)
7. Schandl, S.,, Meyer, F., *A&A*, **289**, 149–161 (1994)
8. Papaloizou, J. C. B.,, Pringle, J. E., *MNRAS*, **202**, 1181–1194 (1983)
9. Papaloizou, J. C. B.,, Lin, D. N. C., *ApJ*, **438**, 841–851 (1995)
10. Brandenburg, A., Nordlund, Å., Stein, R. F.,, Torkelsson, U., *ApJ*, **446**, 741–754 (1995)
11. Hawley, J. F., Gammie, C. F., Balbus, S. A., *ApJ*, **440**, 743–763 (1995)
12. Miller, K. A., Stone, J. M., *ApJ*, **534**, 398–419 (2000)

13. Torkelsson, U., Ogilvie, G. I., Brandenburg, A., Pringle, J. E., Nordlund, Å., Stein, R. F., *MNRAS*, **318**, 47–57 (2000)
14. Shakura, N. I., Sunyaev, R. A., *A&A*, **24**, 337–355 (1973)
15. Stone, J. M., Hawley, J. F., Gammie, C. F., Balbus, S. A., *ApJ*, **463**, 656–673 (1996)
16. Gammie, C. F., Goodman, J., Ogilvie, G. I., *MNRAS*, 318, 1005–1016 (2000)